LCLS-II Technical Note

COUPLER RF KICK IN THE 1.3 GHZ LCLS-II ACCELERATING CAVITY

LCLS-II TN-14-04

1/10/2015

A. Lunin, N. Solyak, A. Sukhanov, V. Yakovlev

1 INTRODUCTION

The 1.3 GHz ILC accelerating structure is chosen as a baseline for the LCLS-II linac. The cavity contains 9 elliptical cells, a main power coupler, and two HOM couplers, upstream and downstream, see Figure 1.

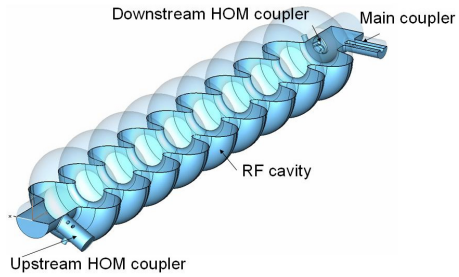

Figure 1 The 1.3 GHz ILC accelerating cavity with main and HOM couplers.

Main and HOM couplers break the cavity axial symmetry, distort electromagnetic field and, thus, create a transverse kick, even for a particle moving along the cavity axes. Dependence of the kick on the RF phase causes beam emittance dilution and may degrade the FEL radiation quality [1, 2]. Bellow we analyze a coupler RF kick in the first accelerating structure of the LCLS-II linac [3]. Beam and cavity parameters relevant to the coupler kick and emittance growth calculations are listed in the Table 1.

Table 1 Parameters for the RF kick and emittance growth simulations.

Bunch transverse size, rms, σ_t	1 [mm]
Bunch length, rms, σ_z	1 [mm]
Input beam energy, E_{inp}	0.75 [MeV]
Accelerating gradient, G	12 [MeV/m]
Operating frequency, F	1.3 [GHz]
Cavity Q-external, Q_{ext}	4E7

2 GENERAL

In order to achieve reliable estimation for the rf kick, we used the following approaches in numerical the electromagnetic analysis: (a) different mesh geometry, (b) different mesh size and (c) a second order of finite elements. All these methods are utilized by the ANSYS HFSS code with a non-uniform tetrahedral mesh [4]. A special three-zone mesh (see Figure 2) was used in order to improve the field approximation near the axis. Intermediate mesh is necessary to match the fine mesh near the axis and regular mesh in the rest of the cavity. The longitudinal component of electric field near the cavity axis is few orders of magnitude larger than the transverse one. Therefore, any misalignment of mesh elements in respect to the axis may result in appearance of a nonzero transverse projection of the longitudinal component and, thus, produce spurious transverse components of electric field. Since a magnetic field is usually derived from the solution of an electric field we have the same problem for an accurate magnetic field representation near the cavity axis. The remedy is use a regularized mesh with the elements aligned to the cavity axis. A regular mesh pattern near the cavity axis and the vertical component of electric field are shown in Figures 3 and 4 respectively as a result of ANSYS HFSS simulation [4]. The calculated EM-fields along the cavity axis are plotted in Figure 5 for electric (a) and magnetic (b) components.

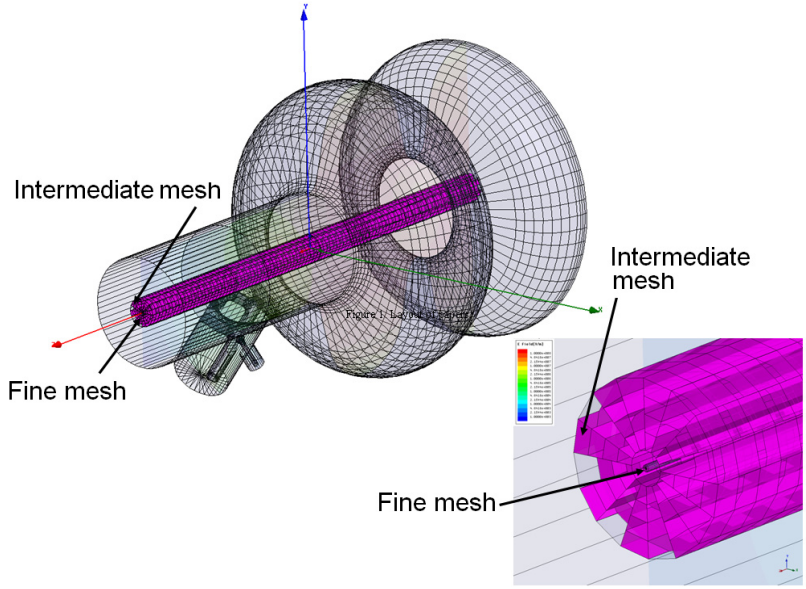

Figure 2: The three-zone mesh for HFSS used in order to improve the field approximation near the axis. Fine mesh repeats the pattern of the intermediate one.

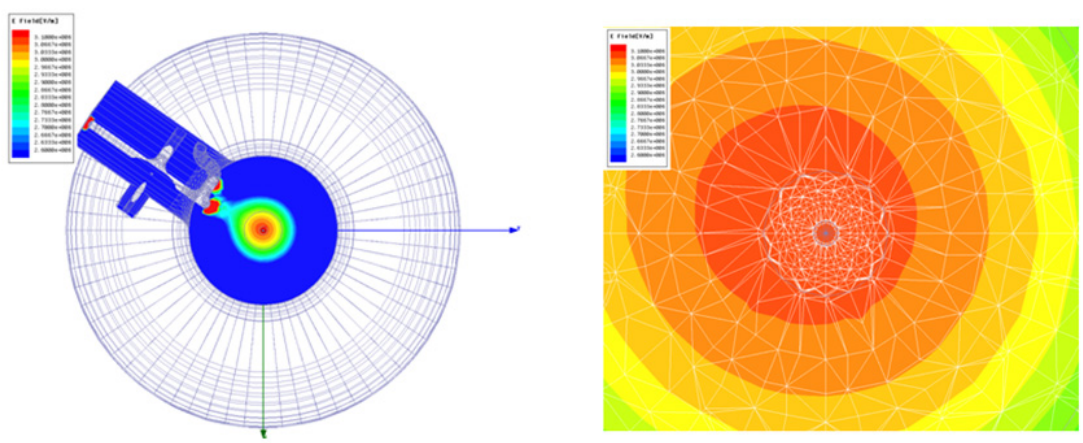

Figure 3: The electric field pattern near the coupler. The field asymmetry causes RF kick.

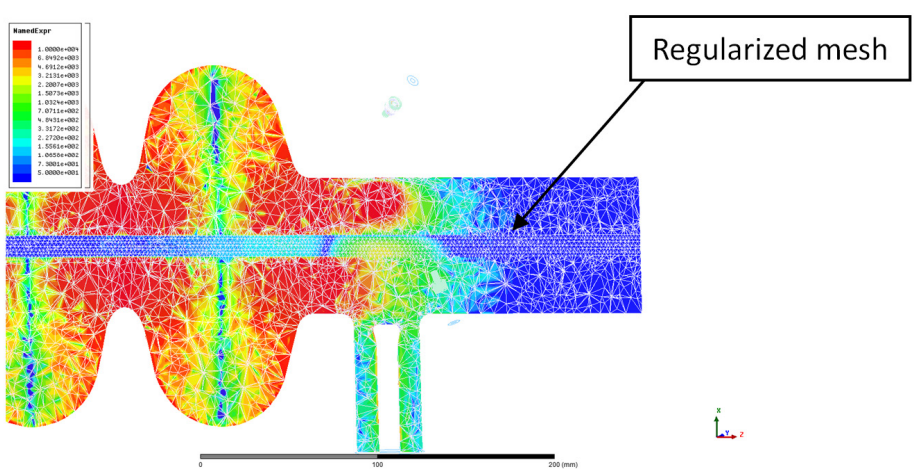

Figure 4: Map of vertical electric field component E_y in the horizontal plane.

The transverse rf kick is the total beam transverse momentum change along the trajectory. For a highly relativistic beam, when trajectories are linear, one can define the normalized transverse kick factor as the complex ratio of transverse and longitudinal momentums by the following way:

$$\kappa_x = \frac{\Delta P_x}{\Delta P_z} = \frac{\int_{z_1}^{z_2} (E_x - Z_0 H_y) e^{i\omega z} dz}{\int_{z_1}^{z_2} E_z e^{i\omega z} dz} \tag{1}$$

where κ_x is a horizontal kick factor, z_1 and z_2 are longitudinal coordinates, E_x, H_y and E_z are complex EM-field components and Z_0 is the impedance of free space. For a low relativistic beam which is moving not along a straight line, dependence of the transverse momentum on the accelerating gradient becomes non-linear. Therefore we characterize RF kick in this case as a non-normalized transverse kick accumulated along the actual beam trajectory at a given accelerating gradient:

$$V_x = \Delta P_x \frac{c}{e_0} = \int_{t_1}^{t_2} (E_x - \beta_z Z_0 H_y) e^{i(\omega t + \varphi_s)} dt \tag{2}$$

where t_2-t_1 is the beam transit time, β_z is the longitudinal beam velocity as a fraction of speed of light, φ_s is the synchronous RF phase, e_0 is electron charge and c is the speed of light. The beam tracking in the accelerating structure is realized with MATHCAD script using the paraxial approximation for particles motion [5, 6]

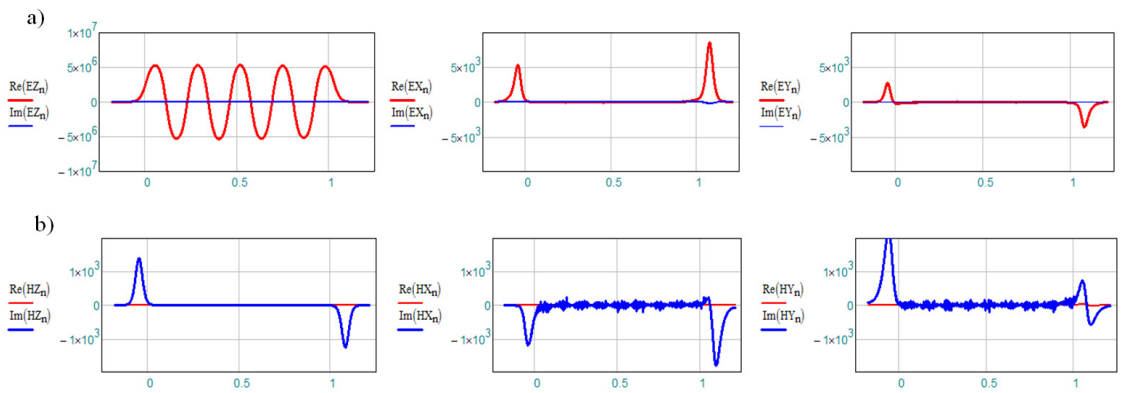

Figure 5 EM-field on the cavity axis, electric (a) and magnetic (b) components.

3 RF KICK IN THE INPUT STRUCTURE OF THE LCLS-II LINAC

A beam RF focusing at the entrance of first accelerating structure, where particles energy is low, is not fully compensated by defocussing forces at its exit [7]. Thus, the structure itself is producing a non-zero net RF kick linearly growing with the beam offset. The main parameter of the cavity RF focusing, which causes beam emittance dilution, is a derivative of the produced transverse voltage over the RF phase. It is weakly dependent on the cavity gradient and falls down rapidly as $\sim\gamma_i^{1.5}$ with the beam input energy.

In order to separate RF kick components produced by structure and couplers, we first simulated RF kick in an ideal structure without HOM and power couplers. The result is shown in Figure 6. The red curve corresponds to the real part of the RF kick and the blue dotted curve represents its phase derivative at the synchronous point. One has to note that for a non-relativistic beam the real and imaginary parts of the RF kick are not exactly cosine and sin functions and, thus, the actual phase derivative of the real part has to be taken into account. A comparison of the imaginary part to the derivative of the real part of RF kick is illustrated in Figure 7 with the difference of about 50% at synchronous phase. Scaling of a cavity RF focusing as functions of the accelerating gradient and the input beam energy are shown in Figures 8 and 9 respectively. For a relativistic approach the real part of transverse voltage is proportional to the cavity gradient and inverse proportional to the energy of the input beam. In the contrary, when the input beam energy is low, the synchronous phase is a function of the cavity gradient and scaling of the cavity RF focusing becomes

substantially non-linear.

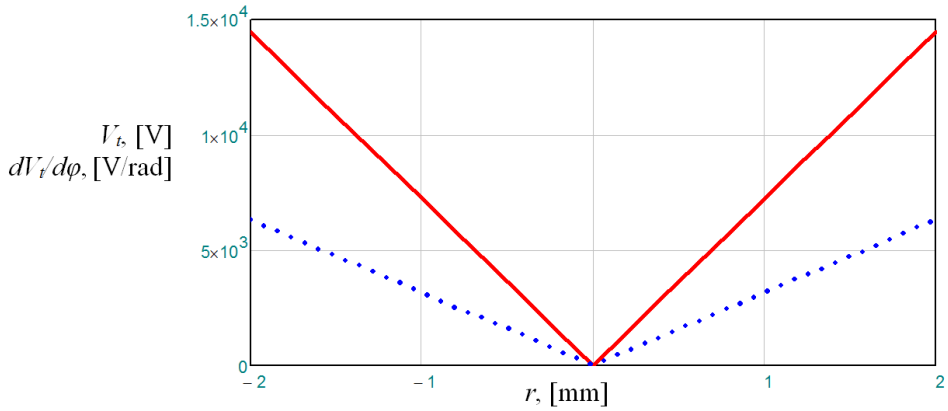

Figure 6 Transverse kick (red curve) and its phase derivative (blue doted curve) in a cavity without couplers.

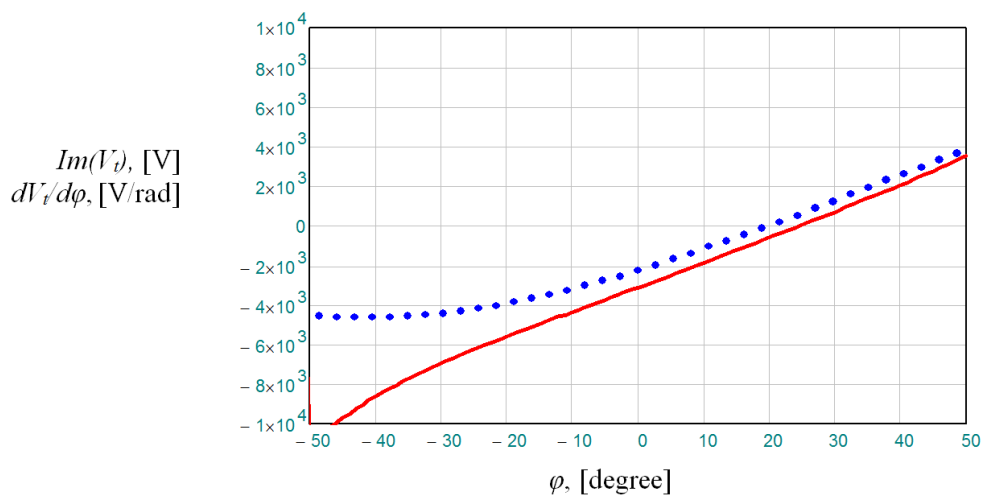

Figure 7 Phase derivative of the real part of the transverse kick (solid red) and its imaginary part (blue doted), where φ = 0 is a synchronous phase.

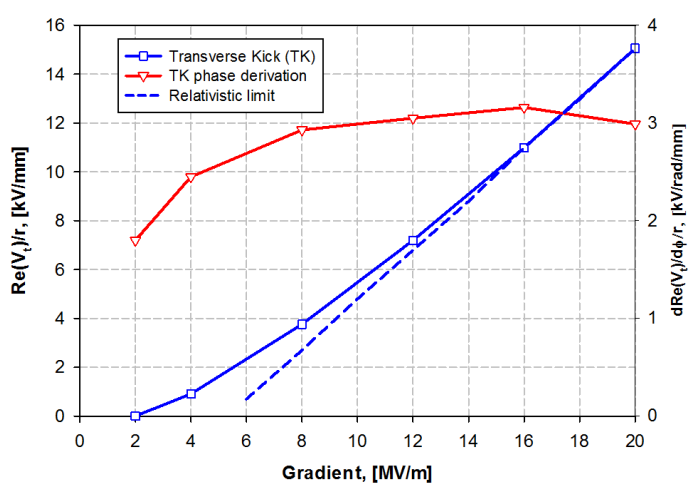

Figure 8 Scaling of a cavity RF focusing versus accelerating gradient, the real part of a transverse kick (blue curves) and kick phase derivative (red).

Adding couplers to the cavity makes the RF kick non-symmetrical in respect to the beam offset. The integrated transverse voltage across the cavity aperture is shown in Figure 10 for the following cases: a)

actual LCLS-II cavity with all couplers, b) cavity with downstream HOM and RF couplers only and c) cavity with upstream HOM coupler only. Since in simulations the total RF kick is a mix of the kicks produced by HOM couplers and by the cavity itself, we have to subtract the cavity background first for restoring kicks produced by upstream and downstream couplers only. The results are illustrated in Figures 11 and 12 for horizontal and vertical components of couplers RF kick accordingly. Both upstream and downstream couplers have kick phase derivatives of the same sign and therefore they do not compensate a beam emittance growth by each other.

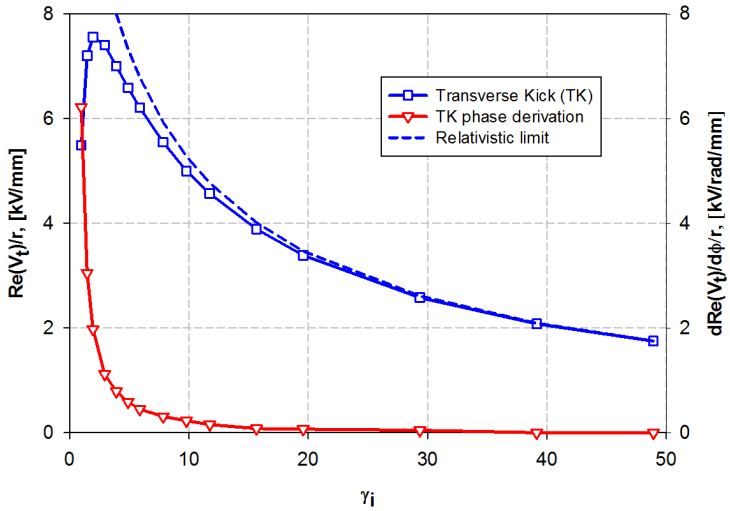

Figure 9 Scaling of a cavity RF focusing versus input beam energy, the real part of a transverse kick (blue curves) and kick phase derivative (red).

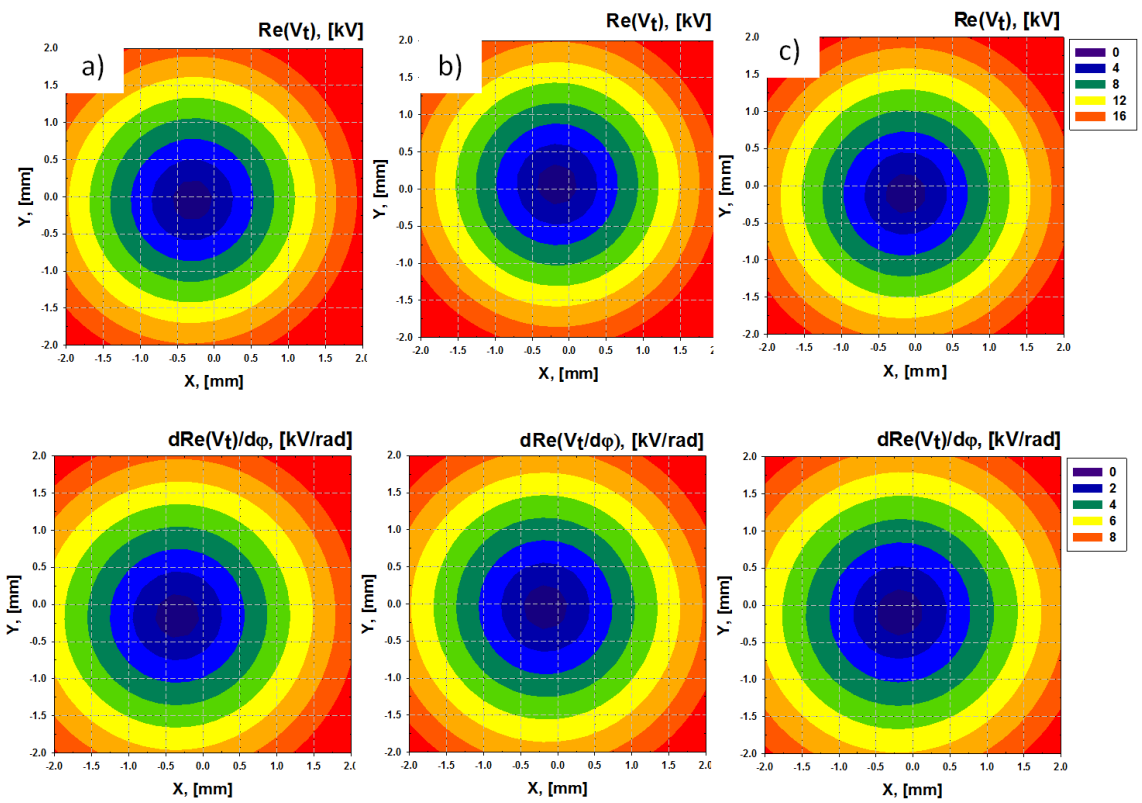

Figure 10 Transverse RF kick (up) and its phase derivative (down) across ±2 mm aperture in the first cavity of LCLS-II linac (a), cavity without upstream HOM coupler (b) and cavity with upstream HOM coupler only (c).

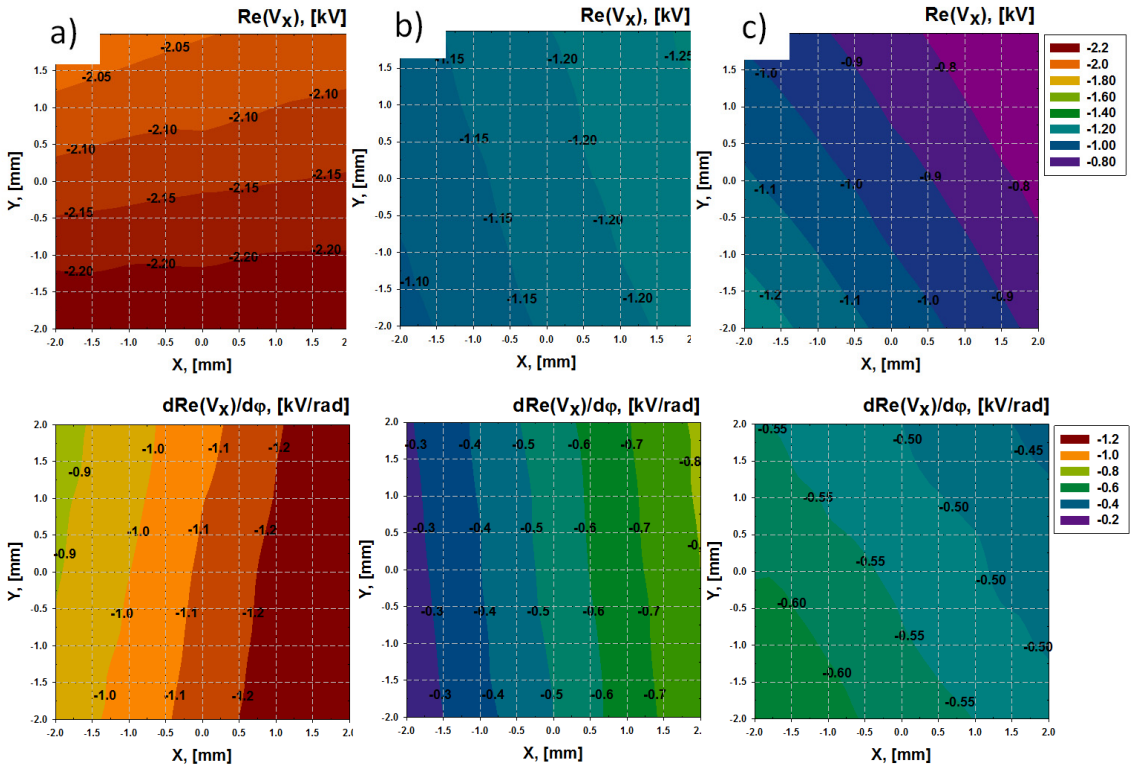

Figure 11 Horizontal couplers RF kick (up) and its phase derivative (down) in the first cavity of LCLS-II linac (a), cavity without upstream HOM coupler (b) and cavity with upstream HOM coupler only (c).

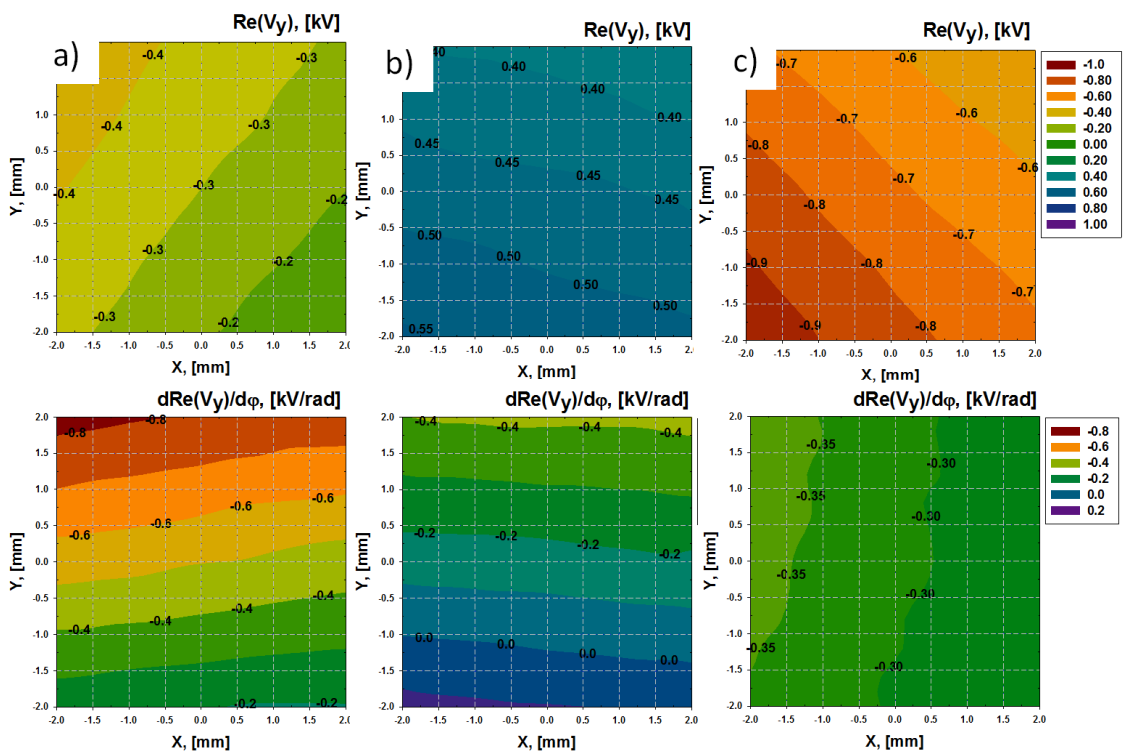

Figure 12 Vertical couplers RF kick (up) and its phase derivative (down) in the first cavity of LCLS-II linac (a), cavity without upstream HOM coupler (b) and cavity with upstream HOM coupler only (c).

Comparisons of the RF kicks produced by the upstream and downstream HOM couplers and the cavity kick due to RF focusing are presented in Figure 13 and Figure 14 respectively. Evidently the effect of coupler

kick outperforms the cavity RF focusing only if the beam offset is less than 0.2 mm in a horizontal plane and 0.1 mm in a vertical plane. It means that if the bunch transverse size or the offset at the moment when it passes near the couplers is greater than 0.2 mm rms, the major portion of the beam emittance dilution will be induced by the structure itself.

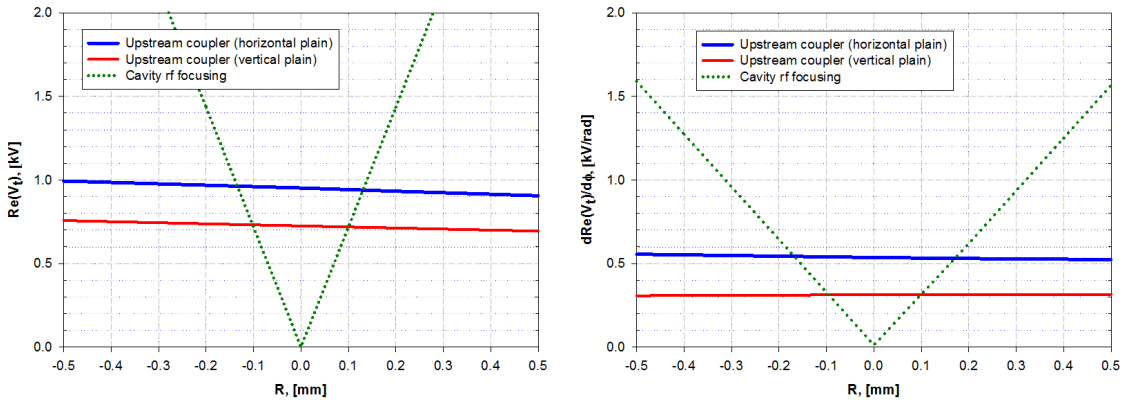

Figure 13 The real part of RF kick (left) and its phase derivatives (right) produced the upstream HOM coupler in horizontal (solid blue) and vertical (solid red) planes and by the cavity (dotted green)

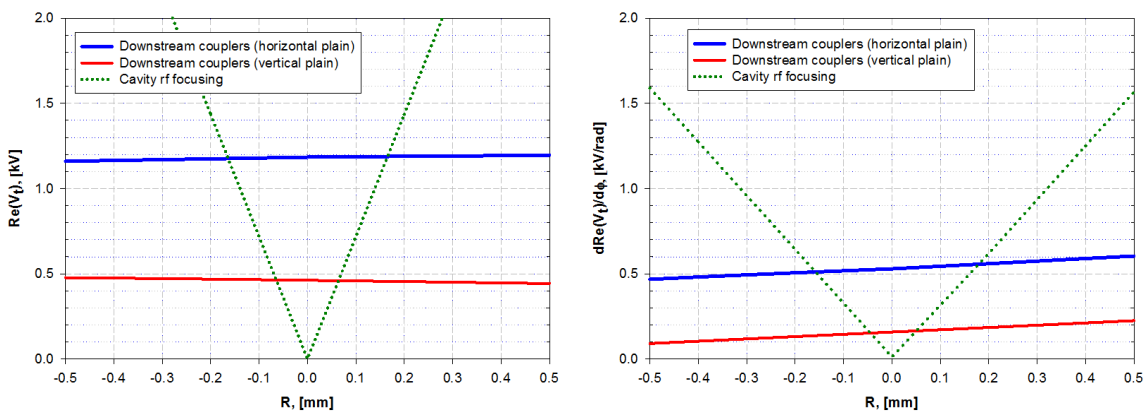

Figure 14 The real part of RF kick (left) and its phase derivatives (right) produced the downstream HOM coupler in horizontal (solid blue) and vertical (solid red) planes and by the cavity (dotted green)

The normalized transverse emittance growth for the Gaussian bunch with parameters listed in the Table 1 can be estimated as follows [8, 9]:

$$d\varepsilon_t = d\sigma_{t'}\sigma_t\beta\gamma \tag{3}$$

$$d\sigma_{t'} = \frac{d\sigma_{p_t}}{p_z} = \left|\frac{dp_t}{d\varphi}\right|_{\varphi=\varphi_0}\frac{k\sigma_z}{p_z} \tag{4}$$

where $d\sigma_{t'}$ is the normalized transverse momentum spread at synchronous phase, σ_t is the bunch size in the transverse plain, σ_z is the bunch length and k is the wavenumber. Using data from Figures 11 and 12, the expected growth of horizontal and vertical emmitanses due to couplers RF kick are about 0.12 mm*mrad and 0.05 mm*mrad respectively.

Finally we calculate dependencies of upstream and downstream couplers transverse RF kicks on the cavity accelerating gradient and the input beam energy. The results are shown in Figures 15 and 16 in a comparison with the effect of RF focusing. One can see that over the wide range of accelerating gradients a phase derivative of the RF kick is dominated mostly by the RF focusing mechanism and the couplers contribution overcomes the cavity part only if the input beam energy is greater than about 5 MeV.

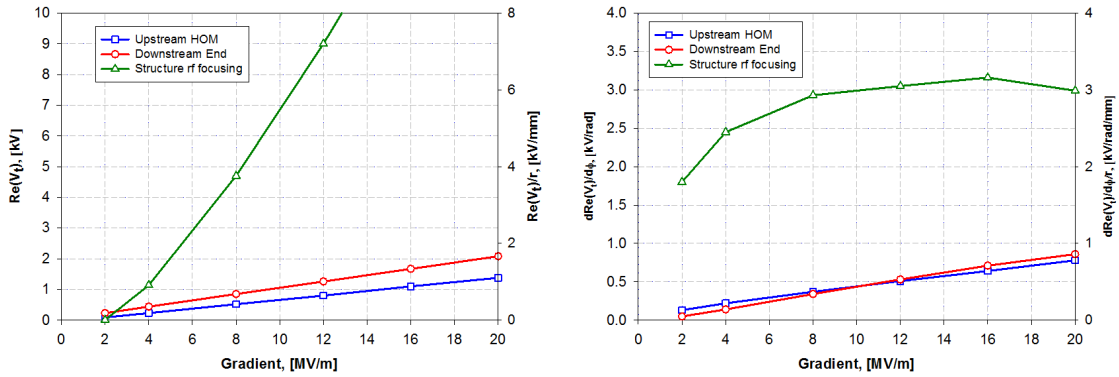

Figure 15 Scaling of the transverse RF kick (right) and its phase derivative (left) as a function of accelerating gradient for the upstream HOM coupler (blue), downstream end couplers (red) and accelerating structure (green).

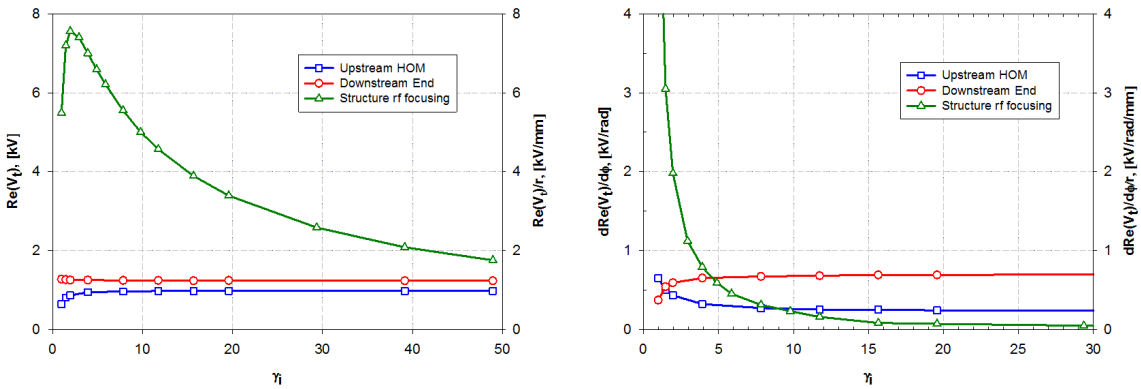

Figure 16 Scaling of the transverse RF kick (right) and its phase derivative (left) as a function of the beam input energy for the upstream HOM coupler (blue), downstream end couplers (red) and accelerating structure (green).

4 RF KICK IN REGULAR SECTIONS OF THE LCLS-II LINAC

Calculation of a coupler RF kick for relativistic beam is a straightforward problem since the structure doesn't produce any transverse kick by itself. Therefore, simple integration over the beam trajectory will give the correct result. The detailed analysis of couplers RF kick for the ILC accelerating structure is presented in [10]. We repeated these simulations using the same approaches for the LCLS-II structure, which has the only difference of a higher external coupling resulted in a smaller penetration of power coupler antenna into the beam pipe. Geometries of ILC and LCLS-II cavities with HOM and power couplers are shown in Figure 17. The offsets of antenna tip are 32.8 mm and 45 mm respectively.

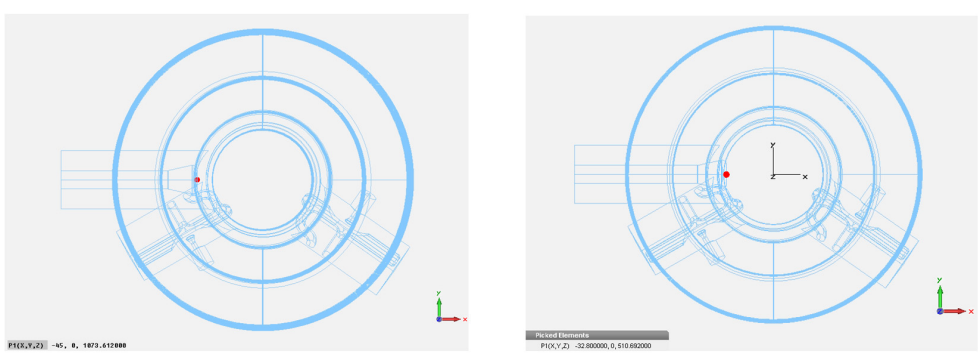

Figure 17 Power coupler antenna penetration for the ILC (left) and LCLS-II (right) cavities.

The result of the couplers RF kick developing along the cavity is illustrated in Figure 18 for electric and magnetic vertical kick components. The kick is shown in the normalized form (1) where the upper integral, representing the change of a transverse momentum, is calculated at each point of the beam trajectory. One can see that the beam sees a transverse kick around the upstream HOM coupler area, and then it remains constant while beam is passing through the cavity and changes again at the exit in a presence of the power coupler and the downstream HOM coupler.

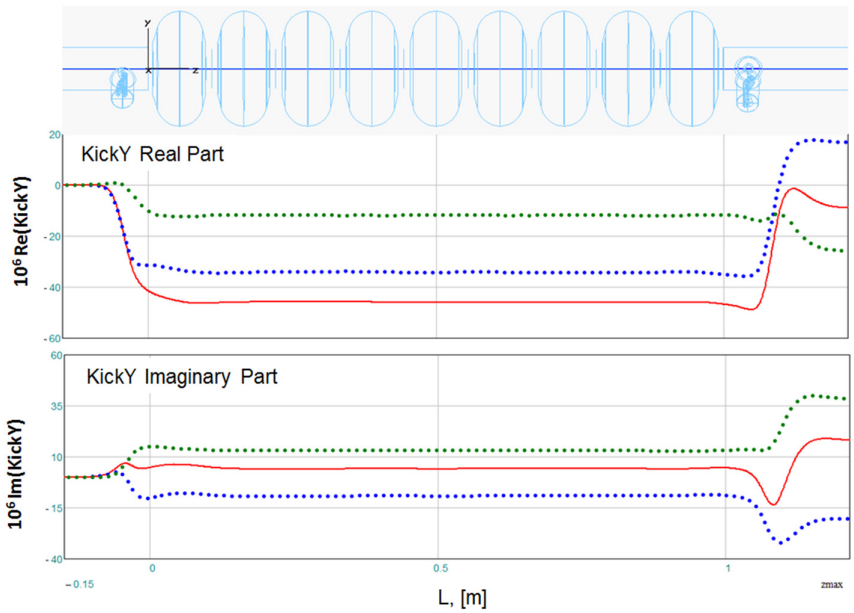

Figure 18 Coupler RF kick simulation. Solid red curve is the full RF kick; dotted blue and green curves are RF kicks produced by electric and magnetic fields.

Since each coupler introduces an asymmetry to the RF field, the beam transverse kick becomes a function of a beam trajectory in respect to the couplers positions. For that we calculated couplers RF kick across the cavity aperture. The results are illustrated in Figure 19 for horizontal and vertical kick components respectively.

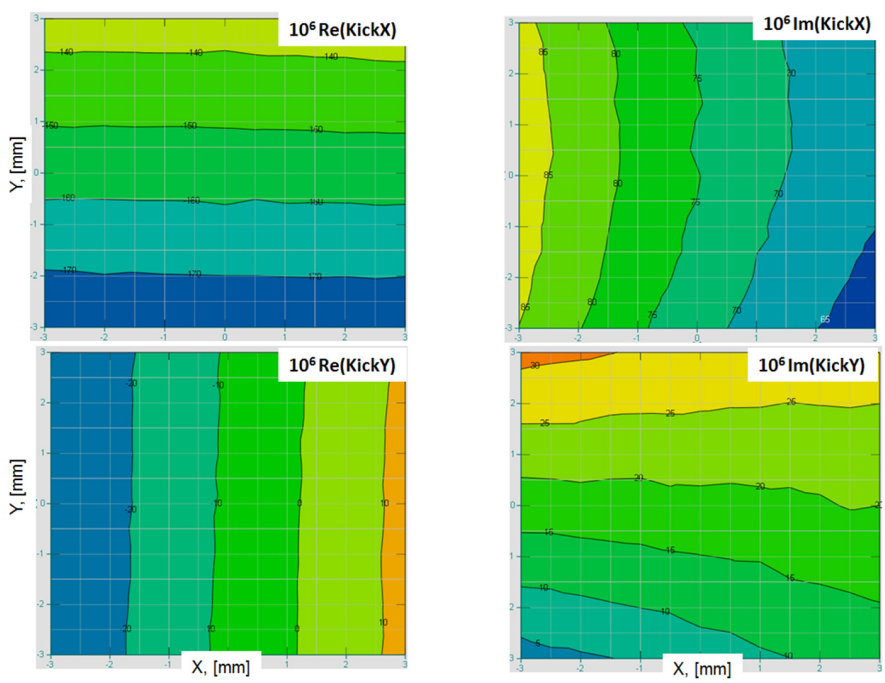

Figure 19 Transverse RF kicks as a function of the beam offset in the 1.3GHz LCLS-II cavity (Q_{ext} = 4E7)

In order to estimate the error of RF kick introduced by the mesh asymmetry we repeated simulation for the cavity with no couplers which should produce zero RF kick in theory. The result is presented in Figure 20 as a normalized ratio of numerical noise and actual coupler RF kick across the cavity aperture. One can see that the relative error of coupler RF kick calculation is below 1% and 5% for horizontal and vertical components.

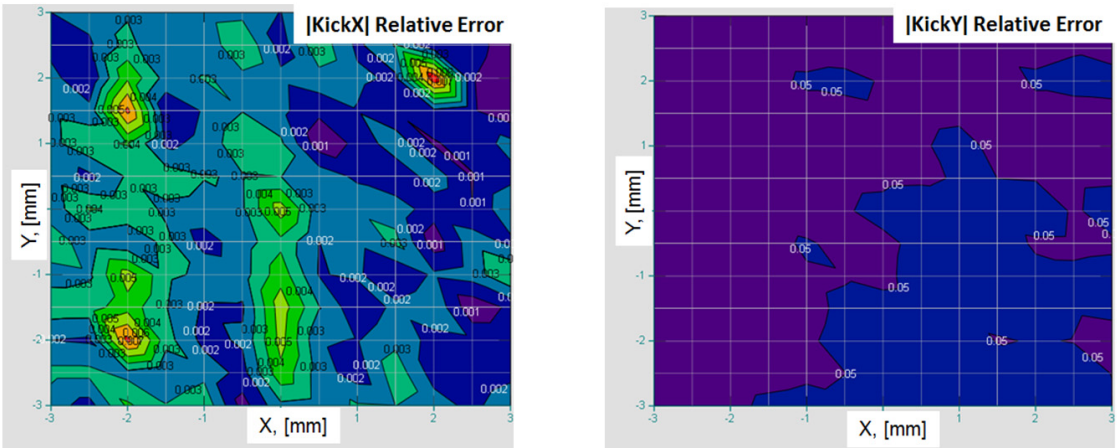

Figure 20 Relative errors of RF kick calculation in the horizontal (right) and vertical (left) planes

The partial RF kicks on the axis produced by the upstream and downstream ends of the structure are summarized in Tables 3 and Table 4 for ILC and LCLS-II configurations respectively. The Panofsky – Wenzel theorem (P/W) was used for crosschecking results of the full RF kick. The module of horizontal component of RF kick in the LCLS-II structure is about 30% larger comparing to the ILC structure as the result of a shallow power coupler antenna penetration into the beam pipe. The vertical component of RF kick doesn't change since geometries of HOM couplers are the same. The real part of RF kick induced either by the HOM or fundamental power coupler is resulted in less than 0.2 mrad beam deflection and, therefore, the couplers satisfy to the LCLS-II 1.3 GHz cryomodule physics requirements of the 3 mrad maximum deflection [11].

Table 3 Couplers RF kick in the ILC 1.3 GHz structure

$Q_{ext} = 3x10^6$	$10^6 \times V_x/V_z$		$10^6 \times V_y/V_z$	
	Direct	P/W	Direct	P/W
Upstream	-64.5 + 19.5i	-	-47.3 + 4.6i	-
Downstream	-34.0 + 65.7i	-	39.4 + 14.9i	-
Full	-99.6 + 82.8i	-98.2+ 85.7i	-7.9 + 19.5i	-6.6 + 17.2i

Table 4 Couplers RF kick in the LCLS-II 1.3 GHz structure

$Q_{ext} = 4x10^7$	$10^6 \times V_x/V_z$		$10^6 \times V_y/V_z$	
	Direct	P/W	Direct	P/W
Upstream	-63.7 + 19.5i	-	-46.1 + 4.5i	-
Downstream	-92.4 + 55.5i	-	37.2 + 13.8i	-
Full	-155 + 75.2i	-156 + 74.5i	-8.9 + 18.0i	-7.8 + 18.8i

5 CONCLUSIONS

Simulations of couplers RF kick in the LCLS-II 1.3 GHz accelerating structure for both ultra-relativistic and non-relativistic regimes are presented. For non-relativistic case scalings of coupler RF kick and cavity RF focusing are compared for various beam input energies and cavity accelerating gradients. The maximum relative error of the RF kick numerical simulation is below 5% because of the used regular mesh. Finaly, we conclude that the 1.3 GHz 9-cell structure can be used for the acceleration of a non-relativistic electron beam while preserving the beam emittance only if it is operating at a low accelerating gradient and proper beam optics is used for minimizing the beam transverse size at the cavity entrance.

6 REFERENCES

[1] A. Latina et. all, ”Study of Coupler’s Effect on ILC Like Lattice”, IPAC 2010, THPD088

[2] Z. Huang, K. Kim, “Review of X-ray Free-Electron Laser Theory”, Phys. Rev. ST AB, 10, 034801, 2007

[3] LCLS-II Conceptual Design Report, LCLSII-1.1-DR-0001-R0, SLAC, 2014

[4] ANSYS HFSS, ANSYS INC, http://www.ansys.com/

[5] http://www.ptc.com/product/mathcad

[6] Yu. Eidelman et. all, “A New Approach to Calculate the Transport Matrix in RF Cavities”, PAC’11, WEP131, New York, NY, USA, 2011

[7] J. Rosenzweig, L. Serafini, “Transverse Particle Motion in Radio-Frequency Linear Accelerators”, Phys. Rev. E, Vol. 49-2, 1994

[8] V. Shemelin, S. Belomestnykh, H. Padamsee, “Low-Kick Twin-Coaxial and Waveguide-Coaxial Couplers for ERL”, Cornell University Report SRF 021028-08 (2002)

[9] M. Zhang and Ch. Tang, “BEAM DYNAMIC ASPECTS OF THE TESLA POWER COUPLER”, Proc. of the PAC1999, New York 1999,pp.2769-2771

[10] A. Lunin et. All, “Final Results on RF and Wake Kicks Caused by the Couplers for the ILC Cavity”, IPAC’10, WEPE034, Kyoto, Japan, 2010

[11] SCRF 1.3 GHz Cryomodule Physics Requirements Document, LCLSII-4.1-PR-0146-R0, SLAC, 2014